

Recoil-distance method lifetime measurements in  $^{173}\text{Ta}$ P. Joshi,<sup>1,2</sup> G. Mukherjee,<sup>2</sup> A. Kumar,<sup>1</sup> R. P. Singh,<sup>2</sup> S. Muralithar,<sup>2</sup> S. K. Chamoli,<sup>1</sup> C. R. Praharaj,<sup>3</sup> U. Garg,<sup>4</sup>  
R. K. Bhowmik,<sup>2</sup> and I. M. Govil<sup>1</sup><sup>1</sup>Department of Physics, Panjab University, Chandigarh 160 014, India<sup>2</sup>Nuclear Science Centre, Post Box 10502, New Delhi 110 067, India<sup>3</sup>Institute of Physics, Bhubaneswar 751 005, India<sup>4</sup>Department of Physics, University of Notre Dame, Notre Dame, Indiana 46556

(Received 1 December 2000; published 1 August 2001)

The nucleus of  $^{173}\text{Ta}$  was populated using the reaction  $^{159}\text{Tb}(^{18}\text{O},4n)^{173}\text{Ta}$  at a beam energy of 84 MeV. Lifetime measurements in the bands built on two Nilsson configurations  $\pi h_{9/2}[541]1/2^-$  and  $\pi g_{7/2}[404]7/2^+$  were performed using the recoil-distance Doppler shift method. The measured lifetimes were used to extract the reduced transition probabilities  $B(E2)$ . Microscopic Hartree-Fock theory with the angular momentum projection was used for calculating the reduced transition probabilities. The  $Q_i$  values obtained from the measured  $B(E2)$  values show a larger collectivity for the  $h_{9/2}$  band as compared to the  $g_{7/2}$  band. Cranked Hartree-Fock Bogoliubov calculations were used for calculating the quasiparticle Routhians. The experimental results in conjunction with the cranking calculations also explain the experimental band-crossing delays associated with the  $i_{13/2}$  neutron alignment in the  $^{173}\text{Ta}$  nucleus.

DOI: 10.1103/PhysRevC.64.034303

PACS number(s): 21.10.Tg, 21.10.Ky, 27.70.+q

## I. INTRODUCTION

The light tantalum isotopes ( $A = 171-175$ ) [1-3] have shown bands built on different Nilsson configurations with contrasting shape driving features. The  $K = 1/2$  band is built on the  $\pi h_{9/2}[541]1/2^-$  configuration. Its energy is highly down sloping with deformation and thus it is supposed to be prolate driving. On the other hand, the bands built on the Nilsson configurations, such as  $\pi g_{7/2}[404]7/2^+$  and  $\pi d_{5/2}[514]5/2^-$ , show a coupled sequence. These coupled bands are characteristic of the higher- $K$  configurations. These configurations are not expected to have a shape driving tendency.

The bands in the tantalum isotopes have shown band crossing which is associated with the alignment of  $i_{13/2}$  pair of neutrons. In general the band-crossing frequency for the alignment of  $i_{13/2}$  pair of neutrons is expected to be independent of the configuration occupied by the odd proton. Therefore, all bands built on different odd proton configurations within the same nucleus are expected to have the same band-crossing frequency. However, if any particular configuration has high deformation driving tendency as compared to the others then the band-crossing frequency gets delayed [4]. The  $K = 1/2$  band in the odd Ta isotopes shows a delayed band crossing compared to the other bands belonging to the same nucleus; therefore one expects a higher deformation for this band. The high  $j$  and low  $\Omega$  configuration coming from the intruder  $h_{9/2}$  level is highly down-sloping as a function of increasing prolate deformation and one expects a stretching of the nucleus along the prolate axis. The band crossing in the  $h_{9/2}$  band in the  $^{173}\text{Ta}$  nucleus [2] takes place at a rotational frequency  $\hbar\omega = 360$  keV. The  $g_{7/2}$  band, built on the  $\Omega = 7/2$  configuration, on the other hand, shows band crossing at a rotational frequency of  $\hbar\omega = 320$  keV. This delay of  $\Delta\hbar\omega = 40$  keV for the  $h_{9/2}$  configuration is an indication of a larger deformation of the nucleus for this configuration.

Since the lifetime measurements of the  $E2$  transitions provide a way of inferring the quadrupole deformation of the nucleus, we have performed lifetime measurements of the levels of these two bands built on  $\pi h_{9/2}[541]1/2^-$  and  $\pi g_{7/2}[404]7/2^+$  configurations in the  $^{173}\text{Ta}$  nucleus.

## II. EXPERIMENTAL DETAILS AND DATA ANALYSIS

Lifetimes were measured in  $^{173}\text{Ta}$  nucleus via the recoil distance method (RDM), using the reaction  $^{159}\text{Tb}(^{18}\text{O},4n)^{173}\text{Ta}$ . The 84 MeV  $^{18}\text{O}$  beam was delivered by the 15UD pelletron accelerator at Nuclear Science Center (NSC), New Delhi. The experiment was performed using the NSC recoil distance plunger device [5] and the Gamma Detector array (GDA). A 1 mg/cm<sup>2</sup> thick target of  $^{159}\text{Tb}$  was stretched and mounted on the RDM device. The stopper was 8 mg/cm<sup>2</sup> gold foil stretched in the similar way and mounted opposite to the target. The distance between the target and the stopper was calibrated using capacitance measurement method [6]. The data were acquired at target-stopper distances ranging from 13 to 10 000  $\mu\text{m}$ . The  $\gamma$  rays were detected with 12 Compton suppressed HPGe detectors of the GDA system arranged in three different rings of four detectors each, and making an angle of 144°, 98°, and 50° with respect to the beam axis, respectively. A 14 element BGO multiplicity filter was also used close to the target site. The data from any of the HPGe detectors were acquired with the condition that at least two of the BGO detectors should fire in coincidence with the HPGe detector. This reduces the background due to Coulomb excitation considerably. The data from all the detectors at one angle were added together to improve the statistics.

The  $\gamma$ -ray transitions deexciting from levels with spin up to  $I^\pi = 25/2^-$  and  $23/2^+$  in the  $h_{9/2}$  band and  $g_{7/2}$  band, respectively, were observed in the experiment. The decay of the levels along a cascade is represented by a set of coupled differential equations called Bateman's equations [7]. The

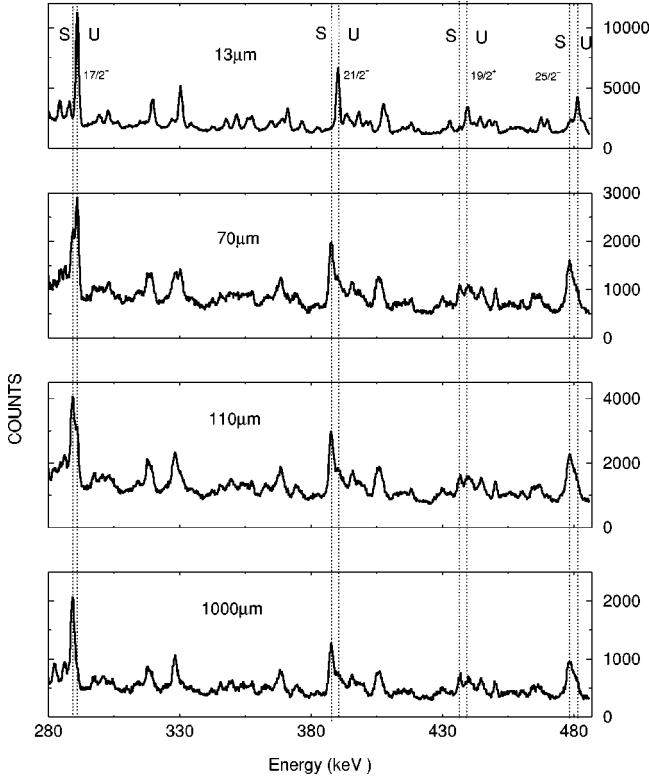


FIG. 1. The shifted (S) and the unshifted (U) peaks for the various transitions in  $^{173}\text{Ta}$  at the backward angle of  $144^\circ$ .

program LIFETIME [8] was used for the present analysis to fit these equations to the experimental decay curves and extract the relevant lifetimes. This program includes the corrections due to the effect of the unknown side feedings. In the present analysis the topmost level of the band being analyzed was assumed to be fed by a rotational cascade comprising of five transitions of known energies. The quadrupole moment for this feeding band was kept a parameter of variation to have the best fit to the observed highest level. The side feedings to all the levels was modeled to have as one step feeding and it was ensured in analyzing each decay curve that the intensity in the band is conserved by the variation of the population from the side feedings. The transition probabilities from the side bands were chosen to have the best fit to the experimental data. The errors were calculated by the subroutine MINUIT [9] of the LIFETIME program which calculates the errors due to the variations of the parameters for the unit change of the chi square. The program LIFETIME also includes the corrections due to the effect of the finite detector solid angle, velocity dependent solid angle, and the alignment attenuation.

### III. RESULTS AND DISCUSSION

#### A. Experimental results

The spectra containing shifted and unshifted partners of the transitions for various target-stopper distances are shown in Fig. 1. The shifted and the unshifted peaks for various transitions were fitted. The normalized intensities of the unshifted components as a function of the target to stopper distance are shown in Figs. 2 and 3 for the transitions of the

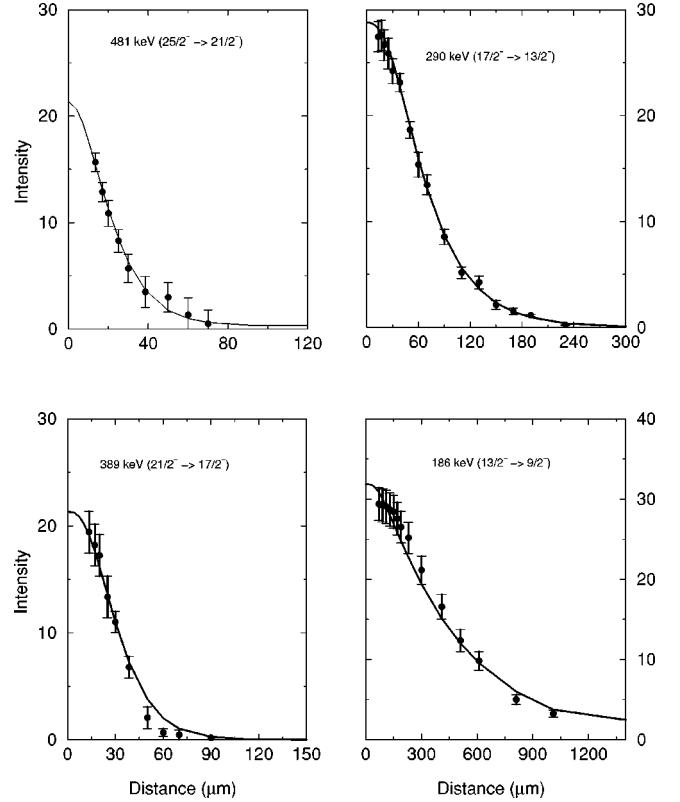


FIG. 2. Decay curves for the unshifted peaks for transitions in the negative parity  $\pi h_{9/2}[541]1/2^-$  band in the nucleus  $^{173}\text{Ta}$ .

$h_{9/2}$  and  $g_{7/2}$  bands, respectively. The fitted lifetimes for  $h_{9/2}$  and  $g_{7/2}$  bands are tabulated in Tables I and II, respectively. The measured lifetimes for different transitions were used to extract  $B(E2)$  values for them. In order to have an idea about the shape of the nucleus for the  $h_{9/2}$  and  $g_{7/2}$  configurations, we extracted the transition quadrupole moments  $Q_t$  using the measured  $B(E2)$  values using the relation

$$B(E2) = \frac{5}{16\pi} e^2 Q_t^2 \langle I2K0 | I-2K \rangle^2 \quad (1)$$

for a transition  $I \rightarrow I-2$  belonging to a band built on a configuration with  $J_z = K$ . These values of  $Q_t$  and the associated deformation parameter  $\beta$  calculated from the experimental  $B(E2)$  values for the  $h_{9/2}$  band and  $g_{7/2}$  band have been plotted in Figs. 4 and 5. The deformations ( $\beta$ ) shown in these figures have been calculated using a linear expansion of  $Q_t$  in terms of the quadrupole deformation parameter ( $\beta$ ) assuming an axial symmetry ( $\gamma = 0^\circ$ ). It is seen from the figures that the  $Q_t$  values for the  $h_{9/2}$  band are  $\sim 15\%$  higher than the  $g_{7/2}$  band. This property of the higher deformation of the  $K = 1/2$ ,  $h_{9/2}$  band compared to the bands built on the other high- $K$  configurations has been observed in  $^{171}\text{Ta}$  [5] also.

#### B. Shape studies using TRS calculations within Hartree-Fock Bogoliubov framework

In order to understand the nuclear shape for  $^{173}\text{Ta}$ , total Routhian surface (TRS) calculations were performed using

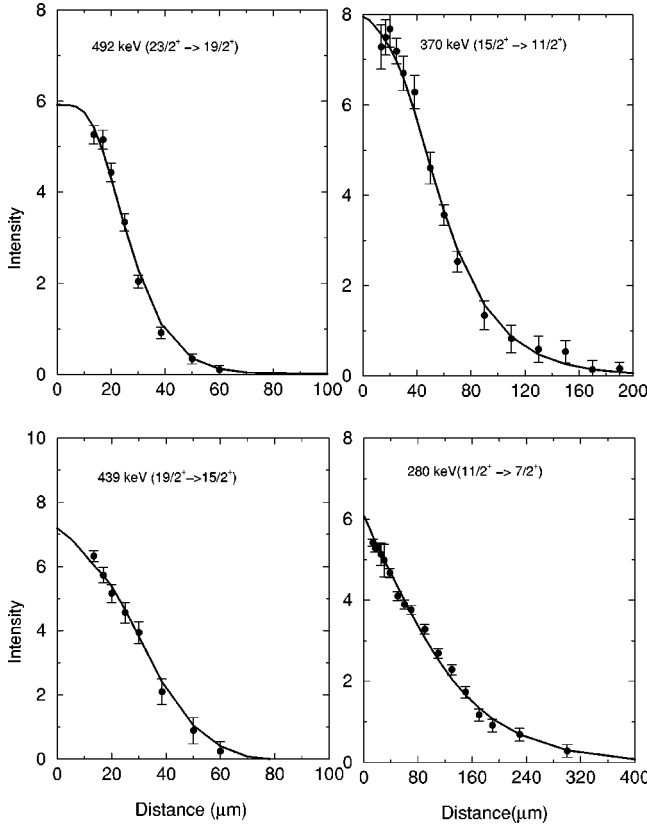


FIG. 3. Decay curves for the unshifted peaks for transitions in the positive parity  $\pi g_{7/2}[404]7/2^+$  band in the nucleus  $^{173}\text{Ta}$ .

Cranked Hartree-Fock Bogoliubov (CHFB) framework [10] with Strutinsky shell correction procedure [11]. The mean field in the calculations was assumed to be of Woods-Saxon [12] type, having a quadrupole as well as a hexadecapole shape. The residual interaction is assumed to be the monopole pairing potential [13] and the pair gap  $\Delta$  and the chemical potential  $\lambda$  were calculated using the BCS self-consistent procedure. The TRS contour plots for the  $-ve$  parity and  $+ve$  signature configuration ( $h_{9/2}$  band) are shown in Fig. 6. The shape of the nucleus defined by the minimum of the contours is close to the value  $\gamma=0^\circ$ . The average deformation parameter calculated from these plots for the  $h_{9/2}$  configuration is ( $\beta\sim 0.28$ ) while the average experimental value of this negative parity configuration ( $h_{9/2}$  band) is  $\beta = 0.32(1)$ , which is about  $\approx 15\%$  higher than the theoretical predictions.

TABLE I. Measured and calculated  $B(E2)$  values for  $h_{9/2}$  band in  $^{173}\text{Ta}$ .

Energy (keV)	Spin ( $I_i^\pi$ )	Lifetime (ps)	$B(E2)$ ( $e^2 \text{b}^2$ )	$B(E2)$ projected HF ( $e^2 \text{b}^2$ )
186	$\frac{13}{2}^-$	$197 \pm_{-9}^{14}$	$1.85 \pm_{-0.12}^{0.09}$	1.98
290	$\frac{17}{2}^-$	$20.0 \pm_{-1.6}^{1.3}$	$1.98 \pm_{-0.12}^{0.17}$	2.01
389	$\frac{21}{2}^-$	$4.29 \pm_{-0.18}^{0.24}$	$2.13 \pm_{-0.11}^{0.09}$	2.12
481	$\frac{25}{2}^-$	$< 1.82$	$> 1.74$	2.16

TABLE II. Measured and calculated  $B(E2)$  values for  $g_{7/2}$  band in  $^{173}\text{Ta}$ .

Energy (keV)	Spin ( $I_i^\pi$ )	Lifetime (ps)	$B(E2)$ ( $e^2 \text{b}^2$ )	$B(E2)$ projected HF ( $e^2 \text{b}^2$ )
284	$\frac{11}{2}^+$	$134 \pm_{-5}^6$	$0.33 \pm_{-0.02}^{0.02}$	0.40
370	$\frac{15}{2}^+$	$13.7 \pm_{-0.6}^{0.7}$	$0.85 \pm_{-0.04}^{0.04}$	0.99
439	$\frac{19}{2}^+$	$4.06 \pm_{-0.64}^{0.42}$	$1.22 \pm_{-0.12}^{0.23}$	1.31
492	$\frac{23}{2}^+$	$< 2.24$	$> 1.26$	1.50

Similar calculations were performed for the  $+ve$  parity and  $+ve$  signature configuration which correspond to the  $g_{7/2}$  band. The results of the TRS calculations for this configuration are shown in Fig. 7. The shape for this configuration is also close to  $\gamma=0^\circ$  indicating the prolate structure. The value of the deformation parameter inferred for this  $+ve$  parity  $+ve$  signature  $g_{7/2}$  configurations is  $\beta\sim 0.27$  which is in good agreement with the average inferred value of  $\beta=0.28(1)$  from the measured  $B(E2)$  values.

In order to see the effect of the different values of the deformations inferred from measurements for the two configurations on the neutron alignment band crossings, we calculated the quasineutron Routhians to find the band-crossing frequency for these two bands. Figure 8 shows the quasineutron Routhians for the nucleus  $^{173}\text{Ta}$  at two different deformations  $\beta=0.32$  and  $\beta=0.28$  which are the average deformations inferred from the measured  $B(E2)$  values for the two bands  $\pi h_{9/2}$  and  $\pi g_{7/2}$ , respectively. The monopole

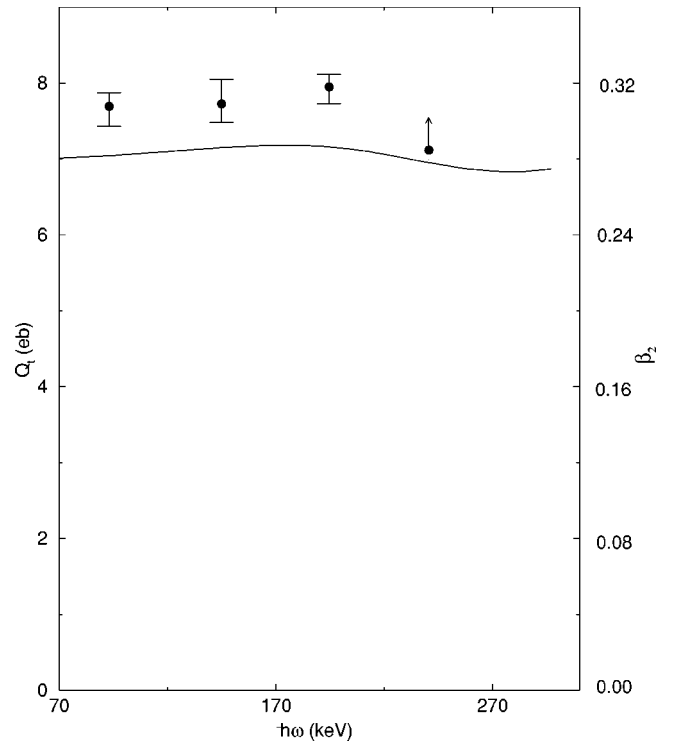


FIG. 4. The extracted  $Q_i$  values from the measured  $B(E2)$  values for the  $\pi h_{9/2}[541]1/2^-$  band of  $^{173}\text{Ta}$  nucleus. The solid curve is the result of the CHFB calculations.

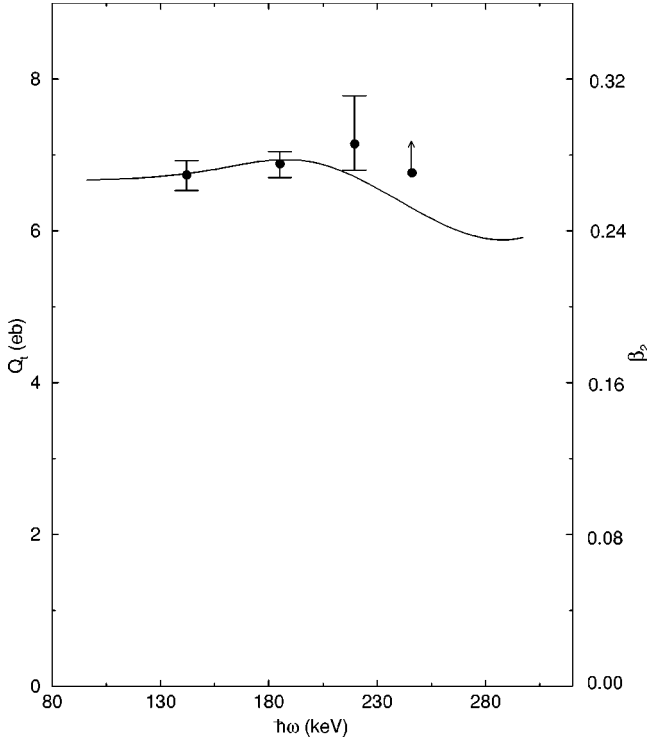


FIG. 5. The extracted  $Q_t$  values from the measured  $B(E2)$  values for the  $\pi g_{7/2}[404]7/2^+$  band in  $^{173}\text{Ta}$  nucleus. The solid curve is the result of the CHF calculations.

pairing used in both these calculations is  $\Delta_n = 1.1$  MeV which is close to the value used earlier [1] for calculating the single quasiparticle Routhians in the  $^{171}\text{Ta}$  isotope. It is clearly visible from the Routhian diagrams that the band-crossing frequency for the neutron alignment increases with increase in deformation. For  $\beta = 0.32$  the rotational alignment of the neutrons takes place at rotational frequency of  $\hbar\omega = 360$  keV, while for  $\beta = 0.28$  the alignment takes place at  $\hbar\omega = 320$  keV. The experimental values of band-crossing frequencies [2] for the  $h_{9/2}$  and the  $g_{7/2}$  bands are 360 and 320 keV, respectively. Thus the experimental delay of  $\Delta\hbar\omega_c = 40$  keV for the  $h_{9/2}$  band as compared to the  $g_{7/2}$  band is reasonably explained using the deformations inferred from the measured  $B(E2)$  values for the two bands.

### C. Microscopic Hartree-Fock calculations with angular momentum projection

In order to investigate the properties of the two bands in  $^{173}\text{Ta}$  the microscopic Hartree-Fock calculations with angular momentum projection were performed. The reduced transition probabilities for the levels of the two bands were calculated in order to compare with the experimental values. The Hamiltonian used in these calculations consisted of a single particle term and a residual two-body interaction term. The closed shells of  $Z=50$  and  $N=82$  were assumed with one major shell active for protons as well as neutrons. A surface delta residual interaction [14] of strength 0.3 MeV was used for  $np$ ,  $nn$ , and  $pp$  type of interactions. This interaction is known to give reasonable deformation properties of the deformed rare-earth nuclei [15]. An axially symmetric

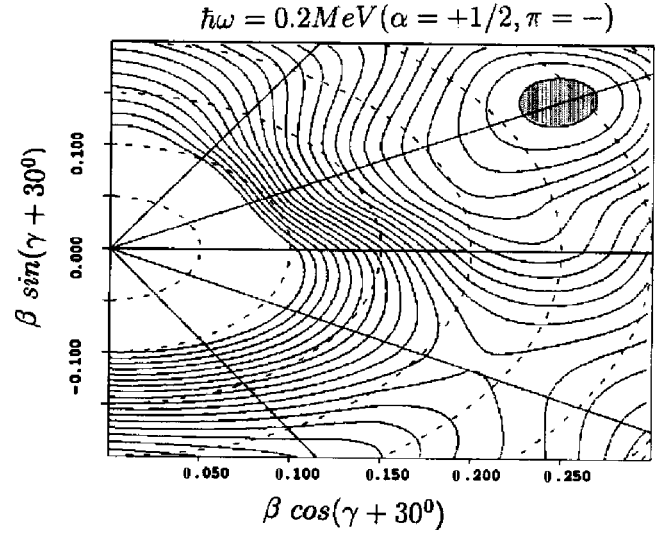


FIG. 6. The TRS plot for the negative parity configuration ( $\pi h_{9/2}[541]1/2^-$  band) in  $^{173}\text{Ta}$  nucleus calculated at a rotational frequency of  $\hbar\omega = 0.2$  MeV.

shape with reflection symmetry was assumed so that configuration mixing occurs only among states of the same  $m$  value and parity  $\pi$ . The band heads for  $K = \frac{1}{2}^-, \frac{7}{2}^+$  bands were generated, respectively, by putting the last proton in  $m = \frac{1}{2}^-, \frac{7}{2}^+$  near the proton Fermi surface. It is to be noted that the  $m = \frac{1}{2}^-$  orbit occupied by the last proton in the  $K = \frac{1}{2}^-$  orbit is predominantly of  $h_{9/2}$  character. The details of the calculations are given elsewhere [5].

The calculated reduced transition probabilities are compared with the experimental values in Tables I and II for the two bands, respectively. An effective charge of  $1.7e$  for protons and  $0.7e$  for neutrons was used in these calculations. These values are the same as used in the other isotope of tantalum, i.e.,  $^{171}\text{Ta}$  [5]. The calculated  $B(E2)$  values for both bands of the nucleus  $^{173}\text{Ta}$  are in good agreement with

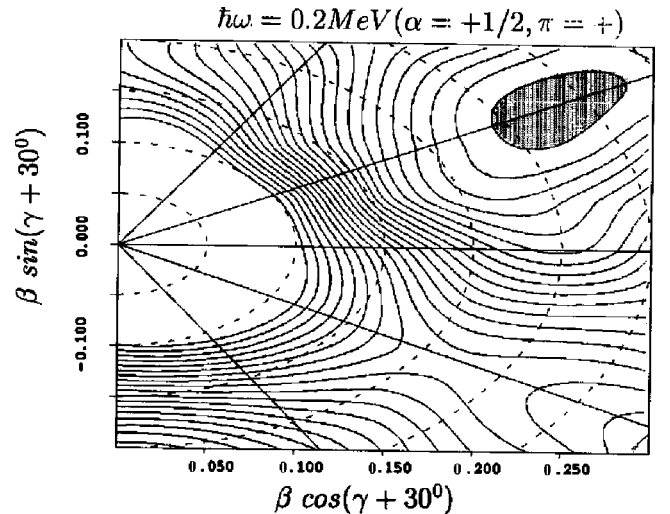


FIG. 7. The TRS plot for the positive parity configuration ( $\pi g_{7/2}[404]7/2^+$  band) in  $^{173}\text{Ta}$  nucleus calculated at a rotational frequency of  $\hbar\omega = 0.2$  MeV.

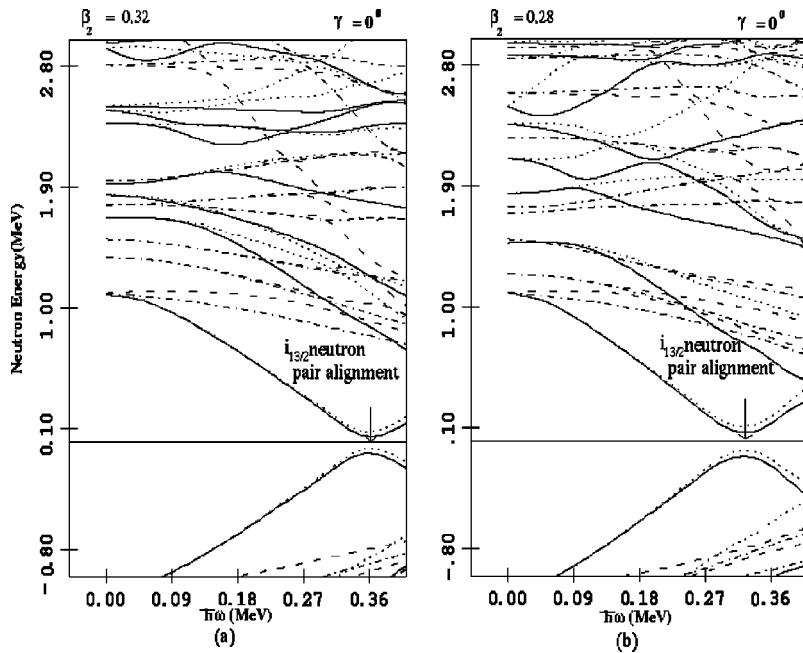


FIG. 8. The quasineutron Routhians describing the delay in the band crossing for the deformed configuration. The two deformations used correspond to the values inferred from the measurements. (a)  $\beta_2=0.32$  for the  $\pi h_{9/2}$  band, (b)  $\beta_2=0.28$  for the  $\pi g_{7/2}$  band. Axial symmetry ( $\gamma=0^\circ$ ) has been used in the calculations.

the experimental results. The constant behavior of the  $B(E2)$  values as a function of spin for the low  $K=1/2$   $h_{9/2}$  band is clearly visible. It is interesting to note that the smoothly increasing trend of the  $B(E2)$  values with spin for the  $g_{7/2}$  band is also well reproduced by the calculations. It is to be noted that the calculated  $B(E2)$  values for the  $h_{9/2}$  band are higher than those for the  $g_{7/2}$  band, as observed experimentally.

#### IV. SUMMARY

Lifetime measurements of the levels of two bands ( $h_{9/2}$  and  $g_{7/2}$ ) in  $^{173}\text{Ta}$  were performed using the RDM technique. The measured lifetimes were used to extract the  $B(E2)$  values and the transition quadrupole moments ( $Q_\nu$ ). The results have shown a larger collectivity for the  $h_{9/2}$  band as com-

pared to the  $g_{7/2}$  band. Microscopic Hartree-Fock calculations were performed with the angular momentum projection to calculate the  $B(E2)$  values. The calculated  $B(E2)$  values are found to be in good agreement with the measured values. The deformations inferred from the measurements have been used for the calculations of the  $i_{13/2}$  neutron pair alignment in the  $h_{9/2}$  and the  $g_{7/2}$  band using cranked Hartree-Fock Bogoliubov formalism. The delay in the band-crossing frequency for the  $h_{9/2}$  band as compared to the  $g_{7/2}$  band has been successfully reproduced from these calculations.

#### ACKNOWLEDGMENTS

The work has been supported in part by the U.S. National Science Foundation (Grants Nos. PHY99-01133 and INT-9215295).

- 
- [1] J.C. Bacelar *et al.*, Nucl. Phys. **A442**, 547 (1985).
  - [2] H. Carlsson *et al.*, Nucl. Phys. **A592**, 89 (1995).
  - [3] W. Shuxian *et al.*, Z. Phys. A **339**, 417 (1991).
  - [4] L.L. Riedinger *et al.*, Nucl. Phys. **A520**, 287c (1990).
  - [5] P. Joshi *et al.*, Phys. Rev. C **60**, 034311 (1999).
  - [6] T.K. Alexander and A. Bell, Nucl. Instrum. Methods **81**, 22 (1970).
  - [7] R. Clark and N. Rowley, J. Phys. G **18**, 1515 (1992), and the references therein.
  - [8] J.C. Wells *et al.*, Report No. ORNL/TM-9105, 1985.
  - [9] F. James and M. Roos, Comput. Phys. Commun. **10**, 343 (1975).
  - [10] R. Bengtsson and J.D. Garrett, in *International Review of Nuclear Physics*, edited by T. England *et al.* (World Scientific, Singapore, 1984), Vol. 2.
  - [11] V.M. Strutinsky, Nucl. Phys. **A95**, 420 (1967).
  - [12] T.R. Werner and J. Dudek, At. Data Nucl. Data Tables **50**, 179 (1992).
  - [13] S.G. Nilsson and I. Ragnarsson, *Shapes and Shells in Nuclear Structure* (Cambridge University Press, Cambridge 1995), p. 290.
  - [14] A. Faessler *et al.*, Phys. Rev. **156**, 1064 (1967).
  - [15] G. Ripka, in *Advances in Nuclear Physics*, edited by M. Baranger and E. Vogt (Plenum, New York, 1968) Vol. I, p. 183.